J Wood Sci (2007) 53:54–60
DOI 10.1007/s10086-006-0820-5

ORIGINAL ARTICLE

Tsutomu Suzuki · Kyoko Suzuki · Yukio Takahashi
Mitsuhiro Okimoto · Tetsuo Yamada · Noriyasu Okazaki
Yuichi Shimizu · Masashi Fujiwara

Nickel-catalyzed carbonization of wood for coproduction of functional carbon and fluid fuels I: production of crystallized mesoporous carbon

Received: August 8, 2005 / Accepted: May 25, 2006 / Published online: October 4, 2006

Abstract Japanese larch wood loaded with nickel (1%–4%) alone or with nickel and calcium (0.25%–1.5%) was carbonized at 800°–900°C for 0–120 min with a heating rate of 5°–20°C min^{-1} in a helium flow of 5.8–46.4 ml STP cm^{-2} min^{-1} to examine the influence of these variables on the crystallization of carbon (the formation of T component) and the development of mesoporosity. From the obtained results, reaction conditions suitable for effective production of carbon with the dual functions of adequate electroconductivity and adsorption capacity in liquid phase were established, thereby explaining the factors that govern the process. It was also confirmed that mesopore having a diameter of about 4 nm was selectively produced at the cost of specific (BET) surface area in parallel with the formation of T component. This result provided good insight into how the simultaneous dual function could be realized.

Key words Nickel-catalyzed carbonization · Crystallized carbon · Mesoporous structure · Dual function

Introduction

Wood is a typical renewable and carbon-neutral energy resource and its conversion into liquid and gaseous fuels has recently grown in importance. Liquefaction and gasification have been attempted mainly in Europe and North America since the oil crisis in the 1970s, and to date many processes have been developed.[1,2] Current technologies are, however, still unsatisfactory in terms of commercial operation. The chief problem lies in the difficulty of obtaining complete and selective conversion into tar (oil) or gases by a single-step thermochemical process, which leads to the total operating cost becoming very high. Thus, it is a commonly held view that full conversion into fluid energies is not always feasible. On the other hand, petroleum resources are predicted to be exhausted in about 40 years.[3] Such predictions, combined with the fact that wood is a high quality biomass, should stress the need for utilization as fluid fuels and as a source of chemicals and materials as substitutes for fossil resources.

Carbonization, which is in principle the same technology as pyrolysis,[4,5] is also a thermochemical energy conversion process from which considerable quantities of oil and gases are obtained. Although the classical technology is inferior to liquefaction and gasification in both yield and fuel quality of the corresponding product, it has industrial advantages of easier operation and lower running cost. Another important point is that the main product, wood char, is widely used particularly in Japan as a soil improver, fodder, moisture conditioner, deodorant, etc., in addition to solid fuel. Thus, while carbonization is an approach that can afford useful solid products, the potential of this technology will remain unexpanded as long as the use of wood char is limited to that of the present state. To raise the value of carbonization, it is necessary to identify new uses for the resulting char along with quality improvements in the derived oil and gases.

From this point of view, nickel-catalyzed carbonization has been developed to determine several functions for the metal-containing wood char obtained at various temperatures: (1) high gasification reactivity of 500°C-char with hydrogen,[6–9] (2) good catalytic activity of chemically modified char prepared at around 600°C in hydrogenation of CO[10] and CO_2,[11] and (3) practical electromagnetic shielding capacity of 900°C-char comprised of electroconductive crystallized carbon (T component).[12] Of these topics, the third may attract the greatest attention because effective crystallization of woody carbon at such a low temperature has not

T. Suzuki (✉) · K. Suzuki · Y. Takahashi · M. Okimoto · T. Yamada · N. Okazaki
Department of Applied and Environmental Chemistry, Kitami Institute of Technology, 165 Koen-cho, Kitami 090-8507, Japan
Tel. +81-15-726-9401; Fax +81-15-724-7719
e-mail: suzuki@serv.chem.kitami-it.ac.jp

Y. Shimizu
Department of Science and Engineering for Materials, Tomakomai National College of Technology, Tomakomai 059-1275, Japan

M. Fujiwara
Graduate School of Engineering, Hokkaido University, Sapporo 060-8628, Japan

been achieved until recently, even though nickel catalyst was used. Furthermore, our recent work[13] disclosed that 900°C-char obtained from Ni 2%-loaded wood was comparable with coal-derived activated carbon[14] in the proportion of mesopore (pore with diameter of 2–50 nm) and specific surface area. It follows that wood carbon having both adequate electroconductivity and adsorption capacity in the liquid phase could be obtained. This is the first finding to simultaneously afford the dual function to carbon materials, thus demonstrating that catalytic carbonization is an innovative method of advanced wood utilization. The aptitude of this process for improving fuel properties of liquid and gaseous fractions will be described in a subsequent article and will strengthen the conviction. However, the optimum reaction conditions, which include the loading of nickel and coloading with calcium to control the activity of the catalyst against the formation of T component,[15,16] to produce such a high value-added wood carbon have not been examined to date. In addition, how the dual function is obtained is still uncertain. These are scientifically interesting topics that deserve investigation.

Under the circumstances, the present study was conducted to examine the influence of reaction variables on the relevant properties of the wood carbon obtained. As a result, suitable reaction conditions were established, thereby identifying the critical factors. The reason for realizing the simultaneous dual function could be elucidated as well. In connection with this situation, it was found that highly selective production of mesopore with a diameter of about 4 nm became feasible. Discussion on these problems will lead to better understanding of this unique catalytic carbonization process of wood.

Experimental

Wood material

Powdered Japanese larch (*Larix leptolepis* Gord) with a particle size range of 0.50–1.40 mm was used as the raw wood material. Its ash content, determined as incombustible residue at 800°C, was 0.15%. The major inorganic components were Ca, Mg, Na, K, Si, and Al, and their amounts were quantified by atomic absorption spectrometric analysis for a sample prepared by dissolving the incombustible residue in aqua regia. The compositions were 42.6%, 14.9%, 6.8%, 11.0%, 14.1%, and 6.2% as CaO, MgO, Na_2O, K_2O, SiO_2, and Al_2O_3, respectively.

Nickel loading and coloading with calcium

As the nickel precursor, nickel acetate [$(CH_3COO)_2Ni \cdot 4H_2O$] was loaded alone or together with calcium acetate [$(CH_3COO)_2Ca \cdot H_2O$] onto raw wood by conventional aqueous impregnation.[6–9,12] Loadings of nickel and calcium were adjusted to 1%, 2%, and 4% and 0.25%, 0.50%, 1.0%, and 1.5 % as metal in wood, respectively. After impregnation, excess water was removed in a rotary evaporator at reduced pressure (20–30 kPa, 30°–40°C). The loading of nickel alone and coloadings of nickel and calcium are hereafter written as "Ni-" and "Ni+Ca-," respectively.

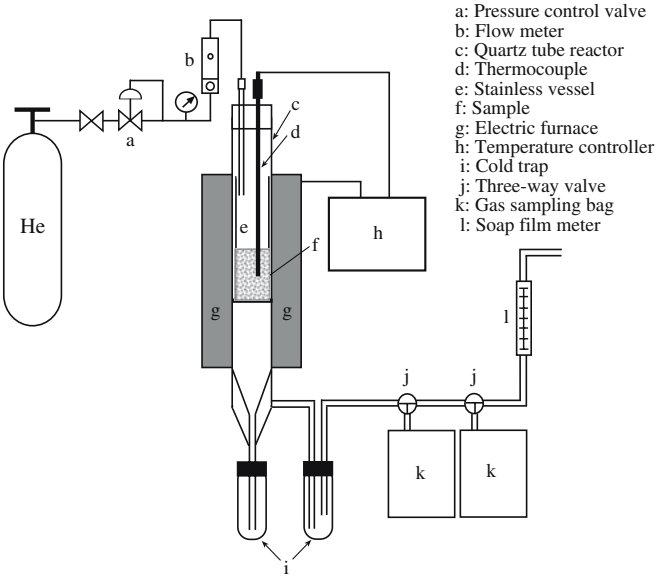

Fig. 1. Reaction apparatus used for nickel-catalyzed carbonization

Carbonization

The reaction apparatus used in this experiment is schematically shown in Fig. 1. About 2 g of Ni-wood or Ni+Ca-wood was packed in a stainless steel vessel and the vessel was placed in a vertical quartz tube reactor. The reactor was then electrically heated at a rate of 5°–20°C min^{-1} in a helium flow of 5.8–46.4 ml STP $cm^{-2} min^{-1}$ to the desired temperature (800°–900°C) and the temperature was maintained for 0–120 min. The same treatment was made with raw wood as reference. Liquid and gaseous fractions produced during the carbonization were condensed in cold traps and collected in sampling bags, respectively, to analyze the composition, as will be described elsewhere. For reaction variables, unless otherwise noted, carbonization temperature, holding time, helium flow, and heating rate were 900°C, 60 min, 23.2 ml STP $cm^{-2} min^{-1}$, and 10°C min^{-1}, respectively.

Crystal structure of carbon, surface area, and pore structure

After weighing to obtain yield on an ash-free, additives-free basis, the resulting char was subjected to measurements of X-ray diffraction (XRD, Rigaku RINT 1200) and adsorption and desorption isotherms of nitrogen at 77 K (ThermoQuest Sorptomatic 1990). In XRD, Cu-Kα ray was radiated to calculate the average crystallite size of carbon indicating the thickness of the hexagonal layer, Lc, and the spacing of the plane, $d002$, from the profile. Peak intensity at the (002) plane was given relative to that of artificial

graphite Lonza and the value expressed as relative peak intensity (RPI) was also employed as a parameter of carbon crystallization. In judgment of the crystallization, practical standards in terms of electromagnetic shielding capacity, 8.5 nm and 15×10^{-3} for *Lc* and RPI, respectively,[13] were adopted. For the nitrogen isotherms obtained, BET[17] and BJH[18] methods were applied to determine BET surface area (SBET), BJH mesopore surface area (Sm), BJH mesopore volume (Vm), and BJH total pore volume (Vt). Volumes occupied by micropore (pore with diameter of <2 nm) and macropore (the diameter >50 nm) were also obtained by the BJH method and they are denoted as Vi and Va, respectively (Vi + Vm + Va = Vt). Data obtained by the BJH method were further used to represent pore size distribution. Parameters employed for evaluating mesoporosity were Sm and Vm, and their standards were settled on 140 $m^2 g^{-1}$ and 0.17 $cm^3 g^{-1}$, respectively, by assuming the application of mesoporous carbon obtained to liquid phase adsorption of macromolecules.[19,20] In addition, Rv, which is defined as the ratio of Vm to Vt, was used to check the selectivity of mesopore as before.[13]

Results

Influence of carbonization temperature and nickel loading

Figure 2 illustrates XRD profiles of 800°-, 850°-, and 900°C-chars obtained from Ni 1%-, 2%-, and 4%-woods. As already stated for Ni 2%-wood,[13] the formation of T component that can be verified by a relatively sharp line at 26° was a little more effective at 900°C than at 850°C and insufficient at 800°C. A quite similar situation was found for Ni 1%- and 4%-woods and thus the three loadings of nickel gave little difference in the peak intensity at each temperature. In Fig. 2, two sharp peaks due to metallic nickel appeared at 44° and 51° for all Ni-chars and their intensities depended upon nickel loading, as is usual. A small peak at about 42° was assigned to another carbon crystallite corresponding to the width of the layer and its intensity was approximately proportional to that of the peak at 26°.

Figure 3A shows isotherms of nitrogen adsorption and desorption for the set of chars in Fig. 2B; Fig. 3B shows the same isotherms for 900°C-chars from three Ni-woods. As is seen in Fig. 3A, a gap between the two curves at about 0.5–0.9 of P/P_0 is wider at higher temperature, implying an increased proportion of mesopore at increased tempera-

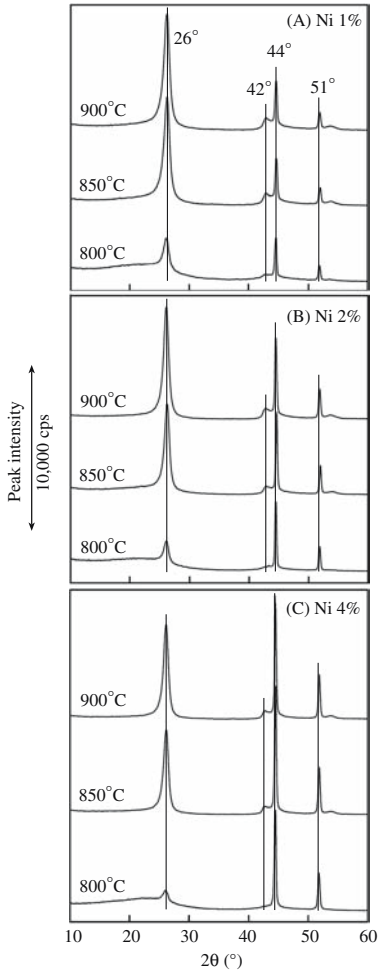

Fig. 2. X-ray diffraction (XRD) profiles of chars obtained by carbonization of **A** Ni 1%-wood, **B** Ni 2%-wood, and **C** Ni 4%-wood at 800°, 850°, and 900°C

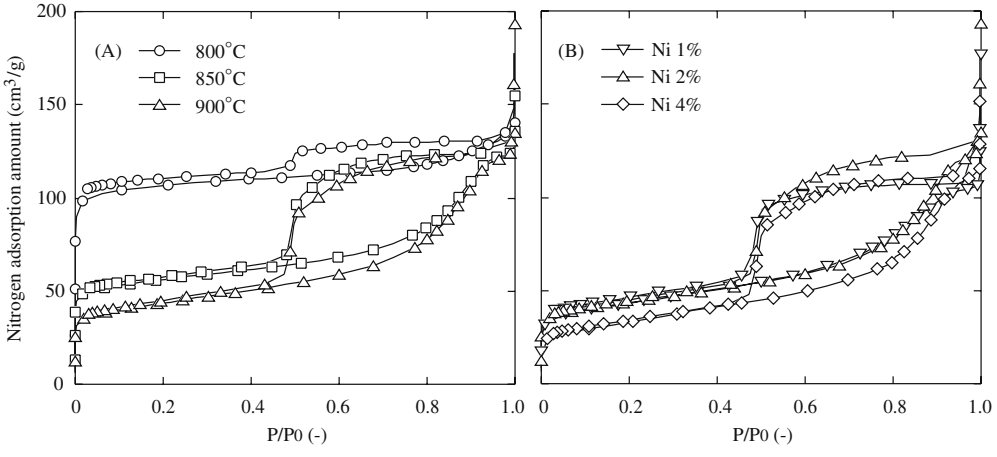

Fig. 3. Nitrogen adsorption and desorption isotherms of **A** chars obtained at 800°, 850°, and 900°C from Ni 2%-wood, and **B** chars obtained at 900°C from Ni 1%-, Ni 2%-, and Ni 4%-woods

ture, although the 850°- and 900°C-chars did not differ greatly. These features analogous to those of the above-mentioned crystallization of carbon were likewise observed for the isotherms of Ni 1% and 4%. That is, difference in mesoporosity among the three Ni-chars was small when the temperature was identical, as can be estimated from Fig. 3B. Figure 4 shows the pore size distributions corresponding to Fig. 3, and these curves manifested that pore diameter converged at about 4 nm regardless of carbonization temperature and nickel loading. This aspect may be more noticeable because to our knowledge, such a narrow distribution of mesopore for carbon materials has never before been obtained. Table 1 summarizes properties relating to crystal structure and pore structure of carbon together with char yield for all Ni-chars, as well as the control chars. Besides the production of amorphous carbon having a small proportion of mesopore by treatment of control char at any temperature, the following are affirmed from the data of Ni-chars: (1) 800°C was too low to attain the above-mentioned standards of *L*c, RPI, Sm, and Vm, (2) 900°C surpassed 850°C in all the values of the four parameters to exceed their standards irrespective of nickel loading, (3) Ni 2% gave larger RPI and Sm than Ni 1% and 4% at 900°C, although it gave smaller Rv. On the grounds of these three points, 900°C and Ni 2% were selected as the appropriate temperature and nickel loading for the production of crystallized mesoporous carbon. Char yield tended to increase with increasing nickel loading, which is in agreement with our previous result,[12] although this aspect is not discussed in this article.

Influence of calcium coloading

According to the decision in the preceding section, 900°C and Ni 2% were selected to investigate the effect of calcium coloading. For comparison, carbonization was performed at 850°C and with the same nickel loading. Figure 5A displays changes of RPI and Vm and Fig. 5B shows those of SBET and Sm with calcium coloading, respectively, for the chars obtained. At both temperatures, RPI and Vm decreased in a nearly identical pattern with increasing amount of calcium. The change of Sm was similar to those of RPI and Vm, whereas that of SBET was opposite. Thus, coloading of calcium helped to increase SBET, thereby retarding the crystallization of carbon and the development of

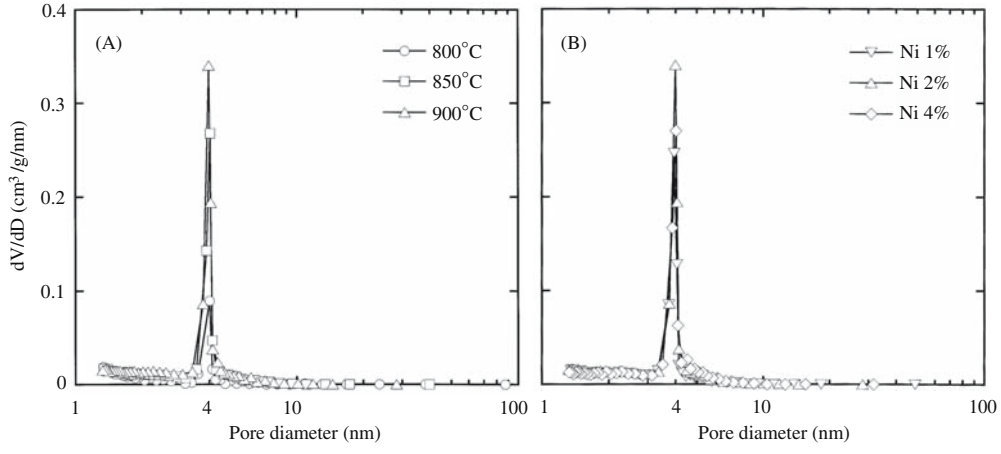

Fig. 4. Pore size distributions of **A** chars obtained at 800°, 850°, and 900°C from Ni 2%-wood and **B** chars obtained at 900°C from Ni 1%-, Ni 2%-, and Ni 4%-woods

Table 1. Yield and properties of none- and three kinds of Ni-chars obtained by carbonization at 800°, 850°, and 900°C

Nickel loading	Carbonization temperature (°C)	Yield[a] (%)	*L*c (nm)	*d*002 (nm)	RPI ($\times 10^{-3}$)	*S*BET (m^2/g)	*S*m (m^2/g)	*V*m (cm^3/g)	*R*v (%)
None	800	24.1	<1.0	–	–	392	26	0.009	13
	850	23.8	<1.0	–	–	288	42	0.020	48
	900	23.8	<1.0	–	–	237	29	0.011	16
1%	800	25.6	9.0	0.342	7.2	327	81	0.055	68
	850	25.5	9.6	0.341	18.3	169	148	0.153	90
	900	25.3	10.1	0.341	23.0	141	156	0.161	77
2%	800	26.0	7.9	0.341	4.9	315	76	0.058	77
	850	25.8	9.8	0.342	19.5	171	162	0.177	79
	900	25.5	10.1	0.342	23.4	140	188	0.203	71
4%	800	27.9	6.3	0.342	3.0	263	68	0.030	52
	850	27.6	9.1	0.342	17.1	177	129	0.168	83
	900	26.7	9.5	0.341	20.7	112	142	0.204	86

*L*c, Average crystallite size of carbon indicating the thickness of the layer; *d*002, spacing of the plane at (002); RPI, relative peak index; *S*BET, BET surface area; *S*m, BJH surface area; *V*m, BJH mesopore volume; *R*v, ratio of *V*m to *V*t (total pore volume) used as the selectivity of mesoporosity

[a] Dry ash-free, additives-free basis

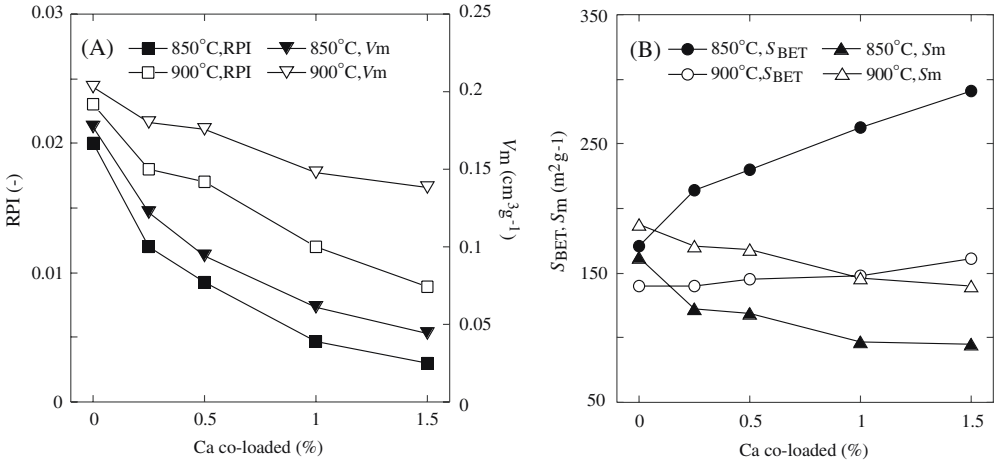

Fig. 5. Changes of **A** relative peak intensity (RPI) and BJH mesopore volume (*V*m) and **B** BET surface area (*S*BET) and BJH mesopore surface area (*S*m) with calcium coloading for Ni-chars obtained by carbonization at 850° and 900°C

Table 2. Influence of helium flow, heating rate, and holding time on the relevant properties of Ni-chars obtained by 900°C-carbonization with 2% nickel

Variables	*L*c (nm)	RPI ($\times 10^{-3}$)	*S*BET (m^2/g)	*S*m (m^2/g)	*V*m (cm^3/g)	*V*a (cm^3/g)	*V*t (cm^3/g)	*R*v (%)
Helium flow (ml STP $cm^{-2}\,min^{-1}$)								
5.8	9.9	20.8	129	171	0.202	0.103	0.309	65
11.6	10.3	22.8	126	184	0.210	0.105	0.316	66
23.2	10.1	23.4	140	188	0.203	0.084	0.287	71
46.4	8.5	21.4	156	148	0.168	0.021	0.187	90
Heating rate (°C min^{-1})								
5	9.5	22.1	131	174	0.186	0.062	0.248	75
10	10.1	23.4	140	188	0.203	0.084	0.287	71
20	9.8	22.8	129	181	0.200	0.090	0.290	69
Holding time (min)								
0	9.3	6.8	305	82	0.047	0.087	0.147[a]	32
30	10.1	19.5	145	176	0.090	0.084	0174	52
60	10.1	23.4	140	188	0.203	0.084	0.287	71
90	11.0	23.9	139	203	0.222	0.104	0.326	68
120	10.9	24.1	122	172	0.210	0.125	0.335	63

Va, BJH macropore volume; Vt, BJH total pore volume = *V*i(BJH micropore volume) + *V*m + *V*a
[a] *V*i was 0.013 cm^3/g, whereas it was <0.001 cm^3/g for other specimens

mesoporosity. This revealed the unfavorable effect of foreign calcium on the formation of both T component and mesopore for wood carbon, although the disadvantage was less serious for carbonization at 900°C. Even in the presence of calcium, convergence of mesopore diameter at approximately 4 nm was observed.

Influence of helium flow, heating rate, and holding time

Table 2 lists data of 900°C-carbonization with Ni 2% to show the effects of helium flow, heating rate, and holding time. At the four different helium flows tested, all of *L*c, RPI, Sm, and Vm satisfied their standards. However, values of these parameters at 11.6 and 23.2 ml STP $cm^{-2}\,min^{-1}$ were larger than those at 5.8 and 46.4 ml STP $cm^{-2}\,min^{-1}$. The suitability of 11.6–23.2 ml STP $cm^{-2}\,min^{-1}$ was also recognized for 850°C and Ni 1% and 4%. Variation of heating rate from 5° to 20°C min^{-1} made no serious difference in the crystal and mesoporous structure of carbon, and satisfactory results were obtained at all three rates. The change of this variable was likewise trivial for other samples, and 10°C min^{-1} was considered adequate. Holding time had a great influence, particularly in the initial period up to 60 min, as was common to all carbonizations. For this reaction system, prolonging from 90 to 120 min induced the transition of mesopore with a diameter of about 4 nm to a macropore to some extent with a little increase of RPI and a small decrease of SBET. A similar change with a loss of the mesopore in this period was found for other systems. The growth into macropore was thus unimportant for the crystallization of carbon, and Sm and Vm, as well as *L*c and RPI, usually reached their maximums at 60 to 90 min.

Relationship between the crystallization of carbon and the development of mesopore

Figure 6 presents plots of SBET, Sm, and Vm against RPI, in which all data are derived from Tables 1 and 2 and Fig. 4. As can be seen from each table and figure, Sm and Vm tended to increase with increasing PRI, while SBET tended to decrease, although the trend appeared to be somewhat different for the absence and presence of foreign calcium.

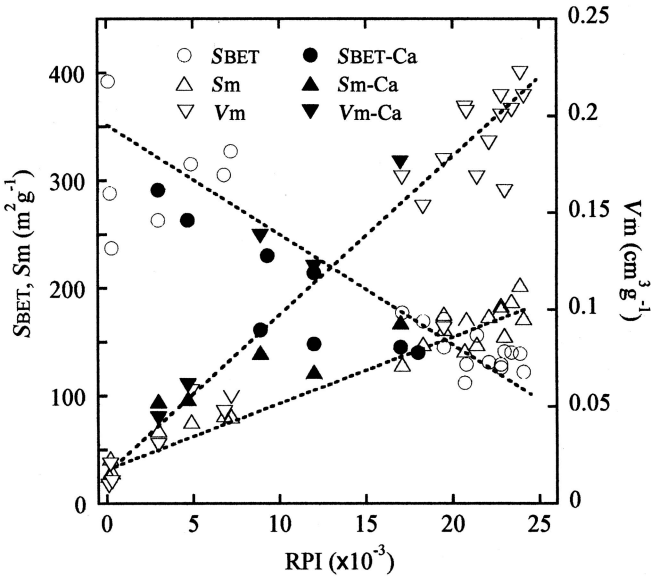

Fig. 6. Relation of *S*BET, *S*m, and *V*m with RPI

As a matter of course, the tendency was unchanged when RPI was replaced by *L*c. It is thus confirmed that the development of mesoporosity featured by highly selective production of mesopore with diameter of about 4 nm had a close relationship with the crystallization of carbon, thereby simultaneously realizing the dual-function wood carbon. It becomes also evident that the increase of mesopore accompanied the decrease of SBET.

Discussion

The foregoing results demonstrated effective production of crystallized mesoporous carbon achieved by the following combination of reaction variables: loading of 2% nickel without calcium, treatment at 900°C for 60–90 min, helium flow of 11.6–23.2 ml STP $cm^{-2}min^{-1}$, and heating rate of 10°C min^{-1}. The results also confirmed a close correlation between the crystallization of carbon and the development of mesopore. It is more significant from technological and scientific viewpoints to clarify the factors that govern the reaction process and how and why the high correlation was found for carbon crystallization and mesoporosity. Discussion is thus focused on these features of the catalytic carbonization with nickel.

As expected, carbonization temperature was a foremost factor in simultaneously obtaining the dual function of wood carbon. Temperature became effective at 850° and 900°C and was independent of the Ni loading (Figs. 2–4, Table 1). This suggested that 850°C would be the approximate lower limit for practical application of the catalysis available, although 900°C was more favorable. It is to be emphasized again that even 900°C is a much lower temperature for crystallizing wood carbon when compared with studies in the literature.[21,22] Although the low-temperature carbonization can be successfully accomplished with the aid of catalytically active nickel, the differences in a number of parameters of the chars for Ni 1%, 2%, and 4% were rather small (Table 1). It appears that Ni 1% provided satisfactory effect and higher nickel loadings were unnecessary. Nickel loadings of 1%, 2%, and 4% on wood amounted to about 4%, 8%, and 15%, respectively, in the resulting char when considering the yield (Table 1). Therefore, Ni 1% was by no means a small loading, but without efficient dispersion of the metal precursor particles within wood tissue, desirable activity cannot be acquired.[12] Excess loading of catalyst, corresponding to Ni 4%, in general brings on worse dispersion, so that catalytic activity is only slightly enhanced or in some cases may be found to decrease. Another possible reason for Ni 4% being inferior to Ni 2%, particularly in the effect on the crystallization of carbon, is degradation of the crystal structure by accelerated gasification.[16] By considering these factors, determination of the appropriate loading of catalyst can be achieved. Although significant differences may be observed for loadings below 1%, the confirmation of such optimization is outside the scope of this study. It was not expected that any coloading of calcium would diminish RPI (Fig. 5A), because its optimum amount for the formation of T component was previously observed for lignin-based char.[16] However, this is not necessarily incomprehensible with wood char. The earlier finding that inherent mineral matter in wood (0.15%) could act adequately as the promoter for nickel catalyst[15] suggests that even 0.25% addition of foreign calcium is excessive. The presence of calcium was coincidently unfavorable for Sm and Vm (Fig. 5). This inconvenience was, however, helpful in corroborating that the production of crystallized carbon and the development of mesoporosity took place at the cost of SBET (Fig. 6) with the diameter of formed mesopore being fixed at almost 4 nm. The decrease of SBETis interpreted as the result of coalescence of micropore into mesopore by considering the relation with Sm and Vm. In fact, this interpretation does not contradict theory of BET[21] or BJH.[22] The coalescence would be induced by the formation of T component, because the crystallite size of 6–11 nm (Tables 1, 2) was compatible with the diameter of mesopore (4 nm). In brief, the formation of the crystallized carbon involves regular structural change by which mesoporosity can be enhanced. It will thus be inevitable that the crystallization of carbon makes SBET decrease. These statements form persuasive argument for the reasons behind the close interrelationship among SBET, Sm–Vm, and *L*c–RPI (Fig. 6). The only exception in terms of the relationship between SBET and Sm–Vm was the decrease of these values by extending the reaction time from 90 to 120 min (Table 2). This observation can be, however, explained by the loss of mesopore once generated from micropore to transform into macropore.

Concerning helium flow, the existence of an optimal value implies that diffusive migration and/or deposition of carbon species on nickel catalyst[23] is an important step for crystallizing carbon and the development of mesoporous structure. That is, 46.4 ml $cm^{-2}min^{-1}$ was too large to promote diffusion and/or a deposition step (Table 2). However, when the flow was in a more favorable range (11.6–

23.2 ml cm^{-2} min^{-1}), this variable had a limited influence. This was also the case with the heating rate. Strictly speaking, the heating rate varied in a moderate range such that it became much less important than carbonization temperature and nickel loading. Nevertheless, adoption of the rate similar to that used in conventional wood carbonization is importance because it ensures easy and simple operation of the nickel-catalyzed carbonization.

In analyzing the influence of holding time, it is interesting to note that part of the mesopore structure was changed into macropore structure in the period of 90–120 min. Although the long latent period for the transition probably reflects the difficult formation of macropore, whether the difficulty is attributed to the activity loss of nickel or low thermal conductivity of carbon remains unclear at present. Why mesopore with diameter of about 4 nm was selectively formed by the nickel-catalyzed carbonization is also left as an unexplainable but interesting phenomenon. Further investigation may be required to fully explain these results.

Conclusions

Nickel-catalyzed carbonization of larch wood was conducted to examine the influence of reaction variables on the crystallization of carbon (the formation of T component) and the development of mesopore. As a result, appropriate conditions were established to effectively produce crystallized mesoporous carbon with electroconductivity and adsorption capacity in the liquid phase. Carbonization temperature was found to be a foremost factor governing the reaction process. It was also confirmed that development of mesopore with a diameter of about 4 nm took place at the cost of BET surface area in parallel with the crystallization of carbon. The close interrelationship of BET surface area, mesoporosity, and crystallized carbon explains how and why the dual function can be achieved simultaneously.

Acknowledgments This work was supported by a Grant-in-Aid for Scientific Research (14560128) from the Ministry of Education, Culture, Sports, Science, and Technology, Japan.

References

1. Bridgwater AV, Czenik S, Piskortz J (2001) An overview of fast pyrolysis. In: Bridgwater AV (ed) Progress in thermochemical biomass conversion. Blackwell, Oxford, pp 977–997
2. Maniatis K (2001) Progress in biomass gasification: an overview. In: Bridgwater AV (ed) Progress in thermochemical biomass conversion. Blackwell, Oxford, pp 1–31
3. Suzuki T (2000) Catalyst technology used in biomass conversion into liquid and gaseous fuels (in Japanese). Shokubai 42:521–525
4. Bridgwater AV, Bridge S (1991) A review of biomass pyrolysis and pyrolysis technologies. In: Bridgwater AV, Grassi G (eds) Biomass pyrolysis liquids upgrading and utilization. Elsevier, London, pp 11–92
5. Elliott DC, Beckman D, Bridgwater AV, Diebold JP, Gevert SB, Solantausta Y (1991) Developments in direct thermochemical liquefaction of biomass: 1983–1990. Energ Fuel 5:399–410
6. Suzuki T, Yamada T, Homma T (1985) Hydrogasification of wood for high heating-value gas production II. Influence of the method of catalyst addition and gasification temperature on CH_4 production (in Japanese). Mokuzai Gakkaishi 31:595–602
7. Suzuki T, Yamada T, Homma T (1992) Hydrogasification of wood for high heating-value gas production VII. Different low temperaure hydrogasification reactivities between wood and bark chars loaded with nickel and iron catalysts. Mokuzai Gakkaishi 38:509–515
8. Suzuki T, Minami H, Yamada T, Homma T (1994) Catalytic activities of ion-exchanged nickel and iron on low temperature hydrogasification of raw and modified birch chars. Fuel 73:1836–1841
9. Suzuki T, Iwasaki J, Tanaka K, Okazaki N, Funaki M, Yamada T (1998) Influence of calcium on the catalytic behavior of nickel in low temperature hydrogasification of wood char. Fuel 77:763–767
10. Suzuki T, Imizu Y, Satoh Y, Ozaki S (1995) High catalytic activity of ion-exchanged nickel on carboxymethylated wood char in methanation of carbon monoxide. Chem Lett 8:699–700
11. Suzuki T (2003) Nickel-catalyzed carbonization of wood for conversion to energy and material (in Japanese). Res J Food Agric 26:20–25
12. Suzuki T, Yamada T, Okazaki N, Tada A, Nakanishi M, Futamata M, Chen HT (2001) Electromagnetic shielding capacity of wood char loaded with nickel. Mater Sci Res Int 7:206–212
13. Suzuki K, Suzuki T, Takahashi Y, Okimoto M, Yamada T, Okazaki N, Shimizu Y, Fujuwara M (2005) Preparation of crystallized and mesoporous carbon by nickel-catalyzed carbonization of wood. Chem Lett 34:870–871
14. Yoshizawa N, Yamada Y, Furuta T, Shiraishi M, Kojima S, Tamai H, Yasuda H (1997) Coal-based activated carbons prepared with organometallics and their mesoporous structure. Energ Fuel 11:327–330
15. Wang XS, Okazaki N, Suzuki T, Funaoka M (2003) Effect of calcium on the catalysis of nickel in the production of crystallized carbon from lignocresol for electromagnetic shielding. Chem Lett 32:42–43
16. Wang XS, Suzuki T, Funaoka M (2004) Production of crystallized carbon for electromagnetic shielding from lignocresol by nickel-catalyzed carbonization. Influence of calcium co-loading (I). Mater Sci Res Int 10:48–52
17. Brunauer S, Emmett PH, Teller E (1938) Adsorption of gases in multimolecular layers. J Am Chem Soc 60:309–319
18. Barrett EP, Joyner LG, Halenda PP (1951) The determination of pore volume and area distributions in porous substances I. Computations from nitrogen isotherms. J Am Chem Soc 73:373–380
19. Fitzer E (1987) The future of carbon-carbon composites. Carbon 25:163–190
20. Nishimiya K, Hata T, Imamura Y, Ishihara S (1998) Analysis of chemical structure of wood charcoal by X-ray photoelectron spectroscopy. J Wood Sci 44:56–61
21. Yasuda H, Tamai H (1996) New porous carbon materials and their adsorption characteristics (in Japanese). Kagakukogyo 4:37–43
22. Tamai H, Kakii T, Hirota Y, Kumamoto T, Yasuda H (1996) Synthesis of extremely large mesoporous activated carbon and its unique adsorption for giant molecules. Chem Mater 8:454–462
23. Shiraishi M (1984) Graphitization of carbon (in Japanese). In: Inagaki M (ed) An introduction to carbon materials. Carbon Society of Japan, Tokyo, pp 29–40